International Journal of Mechatronics, Electrical and Computer Technology (IJMEC)
ISSN: 2305-0543 (Online), ISSN: 2411-6173 (Print)
Vol. 12 (44), Apr. 2022, pp. 5158-5163

Detection of Dynamic Eccentricity Fault in Induction Motors Using Fast Fourier and Wavelet Packet Transform Methods

Mahdi Ahmadi
Department of Electrical Engineering
Esfarayen University of Technology
Esfarayen, Iran
Mahdiahmadi.ee@gmail.com

***Abstract*—This paper presents the effect of rotor dynamic eccentricity fault on the air gap magnetic field and stator current in a tested 3 phase squirrel cage induction motor. The distorted sinusoidal stator current is analyzed by Fast Fourier transform and wavelet packet transform methods to detect the fault. The magnetic fields in the stator, rotor and air gap are simulated using Finite Element Magnetic method. To achieve accurate model, all geometrical, electrical, mechanical, and physical characteristics of different parts of induction motor are considered in the model and the obtained results confirms this issue. To zoom on a particular frequency interval, the wavelet packet transform method is employed. The presented simulation results show although both methods wavelet and Fourier transforms are capable to detect the dynamic fault in the motor, though wavelet transform indicates the fault more clearly.**

***Keywords*— *Dynamic eccentricity, Fast Fourier transform, Fault detection, Induction motor, Wavelet packet transform*.**

I. INTRODUCTION

High cost of unscheduled industrial plant maintenance and the associated repair time, have caused that electric induction motor condition monitoring become crucial in the different industries. Online condition monitoring also increases the reliability and productivity of the machines. For these reasons, recently many researchers have been focused on developing fault detection and diagnosis techniques [1-3].

Early fault detection of large scale induction motors during manufacturing phase can prevent fault propagation in production lines. According to the literature, most of imperative mechanical faults in induction motors are the bearing fault (40%-50%) and eccentricity fault (60%) [4]. Therefore, eccentricity is an important fault for rotary machines which should be mentioned more.

The eccentricity fault causes imbalance air gap between rotor and stator, and hence unbalances the magnetic field. In general three imbalance types of static, dynamic, and mixed eccentricity have been observed and addressed for the squirrel cage induction motors. In dynamic eccentricity, rotational and geometrical centers of the rotor are different and stator center similar to rotational center of rotor. In this case, the minimum distance of air gap is variant with time [5]. Fig. 1 shows the healthy and dynamic eccentricity cases clearly.

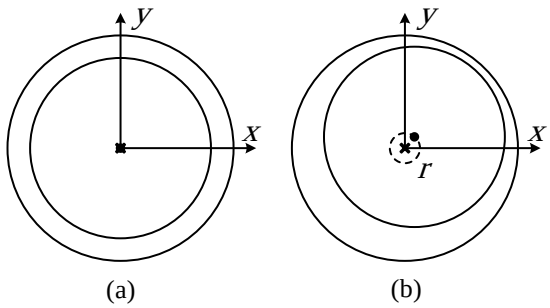

Fig. 1. a) Healthy and b) dynamic eccentricity: • is geometrical center and × is rotational center.

It is important to mention that even in healthy induction motors, due to problems in fabrication and assemblage of parts there is always a percentage of static eccentricity. This can bring about Unbalance Magnetic Pull (UMP) in one direction that may happen to rotor shaft bending, boring, and corrosion on bearings. On the other hand, it is shown that increasing of UMP can lead to dynamic eccentricity phenomenon [6]. Therefore, it is vital to detect this fault in the early stages before making a main failure in the rotary machine.

Since the stator current signal is always available in induction motors and extra sensing elements are not required to measure this signal, analysis of stator current signal is a favorite method among researchers in this field [7]. Moreover, it is proven that dynamic eccentricity fault produces amplitude modulation in the current signal, then its amplitude can be investigated to show the fault occurrence. In this regard, the stator current signal can be analyzed in two cases of transient state and steady-state. In transient state wavelet transform (WT) is usually used and in steady-state case, Fast Fourier Transform (FFT) is more favored. In order to detect the faults using FFT, marginal bands in the corresponding frequency are considered. Also, to detect faults using WT a certain frequency interval should be focused on. This method has been used to detect different faults of induction machines in [8-10]. Among all types of wavelet transforms, wavelet packet transform (WPT) has this feature and can zoom on specific frequency regions [11].

Utilizing finite element method (FEM) for modeling of rotary machines can amend all the weaknesses addressed in

Article History:
Received Date: Nov. 14, 2021, Accepted Date: Jan. 11, 2022, Available Online: Apr. 01, 2022

references [12-15] and provide a precise model in which all geometrical, electrical, physical, and mechanical characteristics are considered. For this reason, the induction motor is simulated by FEM, FLUX 2D software package, in this paper. To tackle with the problem of imbalance in dynamic fault situation, the idea of splitting the air gap into two parts which slips upon each other is used. To detect dynamic eccentricity fault, two methods of FFT and WPT are applied and compared. Based on the obtained results of this research work, although both FFT and WPD methods are able to detect dynamic eccentricity fault, the WPT have significant advantage over FFT. Also, it is shown that small percentages of dynamic eccentricity fault are easily detectable using WPT.

In the following, modeling of healthy induction motor is described in Section 2. After insuring the accuracy of simulation results regarding experimental data in reference [16], dynamic eccentricity fault is studied in Section 3. Two described detection methods, FFT and WPT, are discussed and their results are reported in section 4. Finally, the conclusion of this research is mentioned in Section 5.

II. MODELLING OF INDUCTION MOTOR USING FEM

Technical specifications of the squirrel cage induction motor simulated by FLUX 2D software are listed in Table 1.

Table 1. Electrical and geometrical characteristics of the simulated induction motor.

Characteristic	Value	Characteristic	Value
Rated power	7.5 kW	Outer diameter of stator core	212 mm
Rated source voltage	380 V	Inner diameter of stator core	120 mm
Rated source frequency	50 Hz	Outer diameter of rotor core	119 mm
Number of stator slots	24	Inner diameter of rotor core	40 mm
Number of rotor slots	20	Air gap thickness	0.5 mm
		Length of the stator and rotor core	125 mm

Although, it is possible to model the rotary machines in 3-Dimensional space (3D) by FLUX software, but a 2D model is prepared in this study due to just 2D features of induction motor is enough to reach a high accuracy model. 2D schematic view of the under study induction motor is depicted in Fig. 2. A complete simulation of induction motor by this software package includes several successive steps which are summarized as follows:

- Geometrical simulation: The required parameters, coordinate system, points comprising the smallest extendable surface, parameters of surface extension, meshing and infinity box are defined at this step.
- Defining electrical model: The voltage source, number of rotor bars and their connection arrangement, coils of stator and number of their turns at each phase, resistance and inductance of coils, and so on are defined in this step. Fig. 3 shows the electrical model adopted in this paper.
- Defining physical properties: It is necessary to address physical properties of various parts in this software package. For example, the material of rotor bars should be known in addition to their physical properties such as working temperature, isotropic resistivity and so on. It is also required to define B-H curve which gives the relation between magnetic properties of rotor and stator.

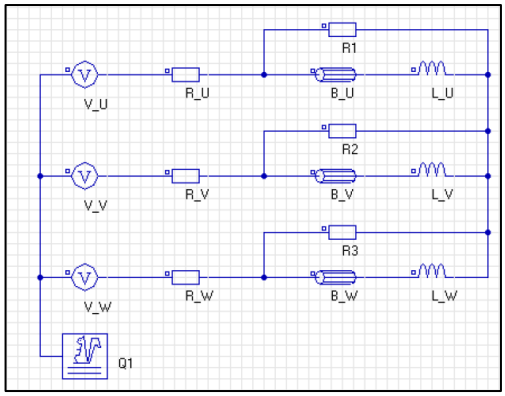

Fig. 3. Electrical model of the induction motor.

- Describing mechanical behavior of parts: When one part of a system has movement, the mechanical behavior of all parts should be exactly determined for the software. This movement can be either rotational or linear.
- Coupling the mechanical and electromagnetic equations: Dynamic behavior analysis of induction motors requires transient magnetic analysis at the presence of electromechanical coupling. In other words, the mechanical equations of rotor's movement are added to either magnetic or electromagnetic modeling. This equation can be generally expressed as follow:

$$J\ddot{\omega} = M_e - M_r - f\,\omega \quad (1)$$

where, J is momentum of inertia, $\ddot{\omega}$ is angular acceleration, M_e is electromagnetic torque, M_r is load torque, f is the friction coefficient corresponding to the mechanical loss, and ω is angular speed. Therefore, coupling the mechanical equations with the electromagnetic equations helps to simulate the dynamic behavior of motor using FLUX 2D and calculate speed and position of rotor at any time step by solving these equations.

In order to investigate validity of the healthy condition modelling, some outputs of our model including angular speed, magnetic torque, and stator current are compared with the results reported in [16] within a compressible air gap. Fig 4 shows the comparison results which confirm that FEM model is effective and the simulation results are reliable.

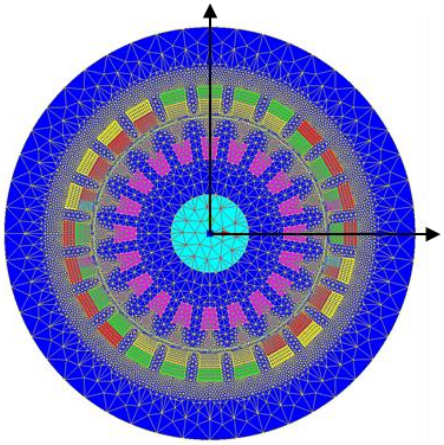

Fig. 2. 2-dimensional view of the induction motor.

IEEE Office - SEET Complex, Federal University of Technology, Owerri, Nigeria, https://aeuso.org
EISSN: 2305-0543, PISSN: 2411-6173

III. Dynamic Eccentricity Fault

There are various fault detection methods for rotary machines, however those are interesting that do not require extra sensors to measure and collect the required data. In this regard, methods based on analyzing the stator current signal are much favored and many researches have been performed to learn the effects of various faults on the stator current signal. To find the dynamic eccentricity effects on the stator current signal, let us consider that length of the air gap $g(\theta,t)$ can be approximated by the following equation for a small air gap and relatively negligible dynamic eccentricity:

$$g_{de}(\theta,t) \approx g_0\left(1-\delta_d \cos\left(\theta-\omega_r t\right)\right) \quad (2)$$

where, δ_d represents the relative degree of dynamic eccentricity, and g_0 is the average length of air gap without eccentricity. This approximation was first introduced by Dorel in 1997 [17]. The air gap permeability $\Lambda(\theta,t)$ is obtained by multiplying $1/g(\theta,t)$ in air permeability μ_0. The following classic method has written the permeability as Fourier series by Cameron and Thomson (1986) [17]:

$$\Lambda_{de}(\theta,t) = \Lambda_0 + \sum_{i_{ecc}=1}^{\infty} \Lambda_{i_{ecc}} \cos\left(i_{ecc}\theta - i_{ecc}\omega_r t\right) \quad (3)$$

where $\Lambda_0 = \frac{\mu_0}{g_0}$ is the permeability without eccentricity. Higher order coefficients of Fourier series can be written as follow:

$$\Lambda_{i_{ecc}} = \frac{2\mu_0\left(1-\sqrt{1-\delta^2}\right)^{i_{ecc}}}{g_0\delta_d^{i_{ecc}}\sqrt{1-\delta^2}} \quad (4)$$

It has been shown that the coefficients are negligible for $\delta_d \le 40\%$ and $i_{ecc} > 2$ [17]. Flux density of the air gap is the product of permeability coefficient in induction driving force (MMF). Total induction driving force can be given by:

$$F_{tot}(\theta,t) = F_1 \cos\left(\rho\theta - \omega_s t - \phi_t\right) \quad (5)$$

where, ϕ_t is the initial phase angle. Therefore, flux density in the presence of dynamic eccentricity will be expressed by:

$$B_{de}(\theta,t) \approx B_1\left(1+2\frac{\Lambda_1}{\Lambda_0}\cos\left(\theta-\omega_r t\right)\right)\cos\left(\rho\theta-\omega_s t-\phi_t\right) \quad (6)$$

where:

$$B_1 = \Lambda_0 F_1 \quad (6)$$

Here, fraction $2\Lambda_1/\Lambda_0$ is almost equal to δ_d for small level of eccentricity. Thus, flux density of the air gap would be rewritten as follow:

$$B_{de}(\theta,t) = B_1\left(1+\delta_d \cos\left(\theta-\omega_r t\right)\right)\cos\left(\rho\theta-\omega_s t-\phi_t\right) \quad (7)$$

This equation indicates the effect of dynamic eccentricity on magnetic flux density of the air gap. The modified airgap permeance causes an amplitude modulation of the fundamental flux density wave with respect to time and space. The amplitude modulation index is approximately the degree of dynamic eccentricity (δ). As a result, amplitude modulation on the stator current can be calculated as follow in the case of dynamic eccentricity.

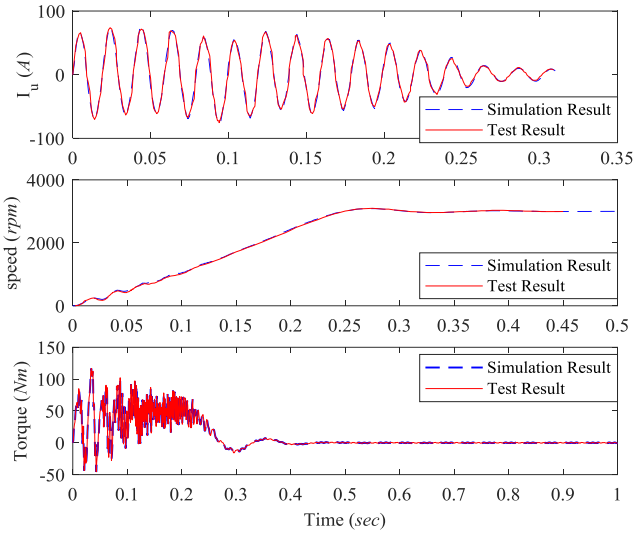

Fig. 4. Stator current, rotor angular speed, and magnetic torque under FEM model and test.

$$I_{de}(t) = I_1\left(1+\alpha\cos\left(\omega_r t\right)\right)\cos\left(\omega_s t-\phi_t\right) \quad (8)$$

where I_1 indicates amplitude of stator current for the fundamental components, α is modulation index of amplitude and is proportional to the degree of dynamic eccentricity (δ_d). Since the stator current signal has two parts of transient and steady states, analyzing it in each of the transient or steady states can result in fault detection propose. FFT and WT are two common methods for analyzing in steady-state and transient, respectively.

IV. Dynamic Eccentricity Fault Detection

A. Fault Detection Using FFT

It is shown that in the case of dynamic eccentricity, the stator current signal consists of the fundamental component and additional side band components [12]. It is should be noticed that amplitude of the side band components varies with the degree of dynamic eccentricity fault. Fig 5 shows the frequency spectrum of the stator current signal around the fundamental component (50 Hz) when 50% dynamic eccentricity has been occurred. As seen in Fig 5, there is no increased amplitude around the fundamental component and the frequency spectrums of the stator current signal are completely matched for both healthy and faulty cases. Therefore, it is necessary to investigate other harmonics components. For this purpose, the frequency spectrum around harmonics 17 and 23 have been illustrated in Figs 6 and 7, respectively.

IEEE Office - SEET Complex, Federal University of Technology, Owerri, Nigeria, https://aeuso.org
EISSN: 2305-0543, PISSN: 2411-6173

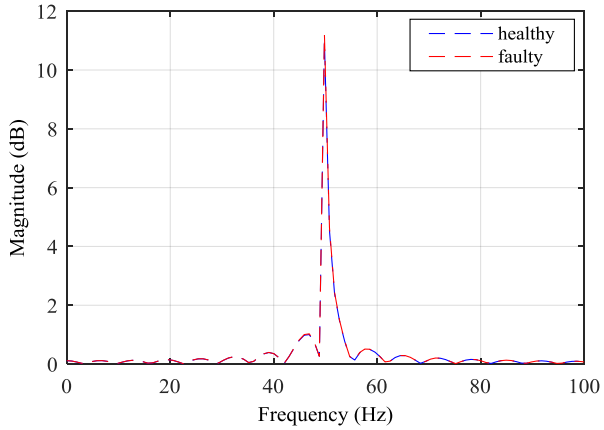

Fig. 5. Frequency spectrum of the stator current signal around the fundamental component (50 Hz) in two cases: Healthy and 50% dynamic eccentricity.

Increased amplitude of side bands around higher order harmonics can be clearly seen in Figs 6 and 7 for the faulty condition. Since amplitude of the stator current signal becomes very small at the higher order harmonics, it is better to utilize the idea of calculating the energy of the signal. Table 2 addresses the energy of the stator current signal around two mentioned harmonics 17 and 23. Although, it is seen that the energy of the stator current signal in the faulty condition is slightly bigger than healthy state and confirms increasing of the side bands' amplitude, but the small value of the obtained energy can mislead the user due to noise effect on the high frequency data.

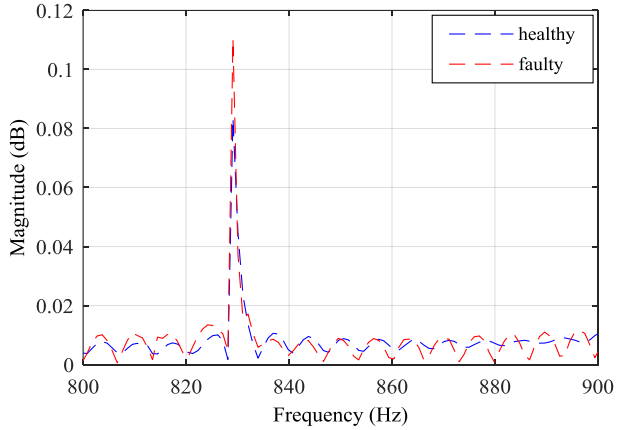

Fig. 6. Frequency spectrum of the stator current signal around the 17th harmonic in two cases: Healthy and 50% dynamic eccentricity.

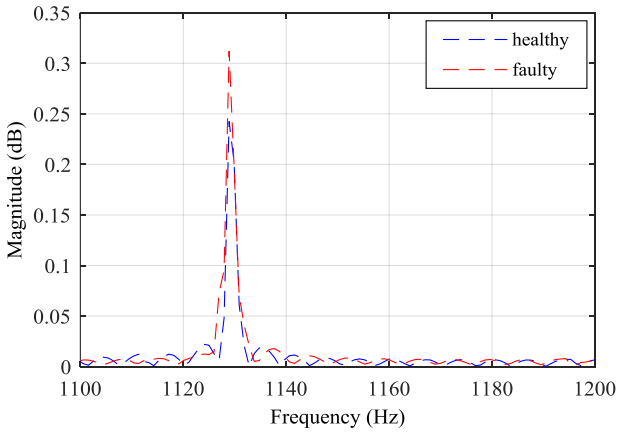

Fig. 7. Frequency spectrum of the stator current signal around the 23th harmonic in two cases: Healthy and 50% dynamic eccentricity.

Table 2. Current signal energy in two cases: healthy and faulty.

Fault Degree		0%	10%	30%	50%
	830	0.055	0.057	0.065	0.066
	1130	0.166	0.169	0.179	0.199

B. Fault Detection Using WT

1) A review of WT theory

As previously explained, WT is the conventional method which analyzes the transient state of signals. Continuous wavelet transform of finite-energy signals ($f(t) \in L^2(r)$) is achieved from the convolution of $f(t)$ with complex conjugate of scaled wavelet $\psi(t)$ as follow:

$$W_f(a,b) = \int_{-\infty}^{+\infty} f(t) \frac{1}{\sqrt{a}} \psi^* \left(\frac{t-b}{a} \right) dt \tag{9}$$

where $\psi(t)$ is the wavelet function, a and b are the transform parameters named Dilation and Translation. The factor $1/\sqrt{a}$ is employed to normalize the wavelet for all a values. As it is known from this equation it can be seen that the wavelet analysis is a time-frequency analysis. Since continues values of a and b increase the amount of calculations, these parameter are usually chosen discrete. A usual choice is $a = 2^j$ and $b = k\,2^j$ in which k and j are integer values. In order to implement a discrete wavelet transform, scaling filter $h(n)$ that is a low pass filter related to scale function $\varphi(t)$ and the wavelet filter $g(n)$ that is a high pass filter related to wavelet function $\psi(t)$ are used as follows [11]:

$$\begin{aligned} \varphi_j(t) &= \sum_k h(k) 2^{\frac{j+1}{2}} \varphi\left(2^{j+1}t - k\right) \\ \psi_j(t) &= \sum_k g(k) 2^{\frac{j+1}{2}} \varphi\left(2^{j+1}t - k\right) \end{aligned} \tag{10}$$

2) A review of WPT

Wavelet packet transform is actually the generalization of WT in which at all stages both low pass filter and high pass filter are split. Therefore frequency precision will be uniform in all regions. It is proven that WPT coefficients in each stage can be computed by [18]:

$$\begin{aligned} d_{j+1}^{2k}(n) &= d_j^k(n) * h(-2n), \quad 0 < k < 2^j - 1 \\ d_{j+1}^{2k+1}(n) &= d_j^k(n) * g(-2n), \quad 0 < k < 2^j - 1) \end{aligned} \tag{11}$$

In wavelet transform tree, the scale parameter (depth) is demonstrated by j, and frequency parameter (node) by *2k* and *2k+1*. The energy of WPT coefficients at each node can be calculated by:

IEEE Office - SEET Complex, Federal University of Technology, Owerri, Nigeria, https://aeuso.org
EISSN: 2305-0543, PISSN: 2411-6173

$$E = \sqrt{\frac{\sum_{i=1}^{M}\left(d_j^k(i)\right)^2}{M}} \quad (12)$$

where M is the number of samples at the node.

3) Dynamic eccentricity detection using Wavelet

In this study, stator current signal measured in various dynamic eccentricity conditions is first decomposed into sub-bands at predetermined levels using WPT algorithm. Then, faulty frequency regions are determined, and coefficient energies in related nodes are calculated. In comparison with a healthy condition, energy is increased in the nodes related to faulty frequency regions due to amplitude modulation of stator current signal, therefore it can be used as a fault index. Fig 8 shows the fault detection procedure using WPT.

In this research, the sampling frequency is $4KHz$ and by utilizing WPT it is divided into 10 levels and the coefficient are obtained. Therefore interval $0-4000$ Hz is divided into 1024 intervals with 3.90625 Hz frequency resolution. As previously deduced, two frequencies 830 and 1130 Hz should be studied to decide that fault has been occurred or not. To this end, energy of the related nodes have been calculated and reported in Table 3. From Table 3, the node's energy increases when the eccentricity fault degree increases. Fig 9 shows the ability of WPT to distinguish the eccentricity fault conditions. It can be seen that dynamic eccentricity fault is more distinguishable when WPT has been employed; especially when a fault with large degree (>30%) happens while the small values of energy obtained by FFT method cannot help the user to distinct between faulty and noisy conditions. Moreover, it is seen that WPT can detect the dynamic eccentricities with small degree (<30%) better than FFT method. Therefore, it can be deduced that dynamic eccentricity affects on the stator current signal such that the steady-state and transient state analysis methods can be employed to detect the fault and its level degree. Meanwhile, the presented results in this paper shows that WPT is more able than FFT to distinguish the faulty cases.

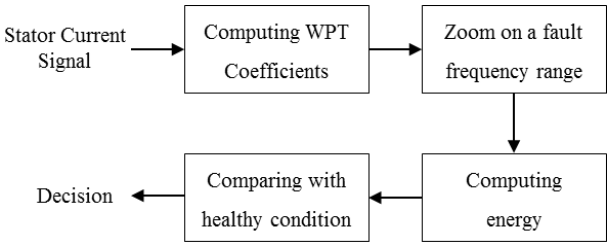

Fig. 8. Fault detection procedure using WPT.

Table 3. Comparison of nodes' energy around 830 and 1130 Hz.

Condition	Frequency Range	
	830 Hz Node (212-214)	1130 Hz Node (289-291)
Healthy	3.3901	1.1727
Fault (10%)	3.6734	1.528
Fault (30%)	3.8263	1.7425
Fault (50%)	4.5521	3.3557

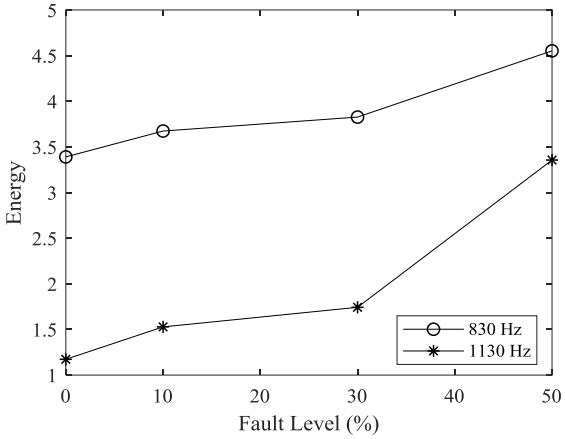

Fig. 9. Energy of nodes around 830 and 1130 Hz.

V. Conclusion

Dynamic eccentricity fault of induction motors has been studied in this work. To simulate the rotary machine, FLUX 2D software has been used which is a finite element method software package. The healthy condition outputs such as stator current, angular speed, and magnetic torque confirmed the modelling accuracy. Then stator current signal has been used to analysis the faulty conditions. Two common methods FFT and WPT have been employed to analysis the steady-state and transient state of the current signal, respectively. The results of our analysis indicate that both methods could detect dynamic eccentricity faults; however WPT is much better than FFT due to its ability to zoom on specific frequency ranges. As a result, dynamic eccentricity faults with small level degree could be detected as well as large level degree faults when WPT is employed.

References

[1] A. Bellini, F. Filippetti, C. Tassoni, and G.A. Capolino, "Advances in Diagnostic Techniques for Induction Machines," *IEEE Transactions on Industrial Electronics*, vol. 55, no. 12, pp. 4109-4126, 2008.

[2] S. Grubic, J.M. Aller, B. Lu, and T.G. Habetler, "A survey of testing and monitoring methods for stator insulation systems in induction machines," in *International Conference on Condition Monitoring and Diagnosis (CMD)*, pp. 196-203, 2008.

[3] H.A. Toliyat and G.B. Kliman, *Handbook of Electric Motors*. Marcel Dekker, 2004.

[4] J. Faiz, B.M. Ebrahimi, B. Akin, and H.A. Toliyat, "Finite-Element Transient Analysis of Induction Motors Under Mixed Eccentricity Fault," *IEEE Transactions on Magnetics*, vol. 44, no. 1, pp. 66-74, 2008.

[5] S. Nandi, H.A. Toliyat, and L. Xiaodong, "Condition monitoring and fault diagnosis of electrical motors-a review," *IEEE Transactions on Energy Conversion*, vol. 20, no. 4, pp. 719-729, 2005.

[6] S. Nandi, R.M. Bharadwaj, and H.A. Toliyat, "Performance analysis of a three-phase induction motor under mixed eccentricity condition," *IEEE Transactions on Energy Conversion*, vol. 17, no. 3, pp. 392-399, 2002.

[7] N. Mehala, "Condition monitoring and fault diagnosis of induction motor using motor current signature analysis," Doctor of philosophy thesis, Electrical Engineering, National Institute of Technology Kurukshetra, India, 2010.

[8] I.P. Georgakopoulos, E.D. Mitronikas, A.N. Safacas, and I.P. Tsoumas, "Detection of eccentricity in inverter-fed induction machines using wavelet analysis of the stator current," in *2008 IEEE Power Electronics Specialists Conference (PESC)*, pp. 487-492, 2008.

[9] G.A. Jimenez, A.O. Munoz, M.A. Duarte-Mermoud, "Fault detection in induction motors using Hilbert and Wavelet transforms," *Electrical*

IEEE Office - SEET Complex, Federal University of Technology, Owerri, Nigeria, https://aeuso.org
EISSN: 2305-0543, PISSN: 2411-6173

Engineering, vol. 89 , no. 3, pp. 205-220, 2007.

[10] H. Hamidi, A.R. Nasiri, and F. Nasiri, "Detection and isolation of mixed eccentricity in three phase induction motor via wavelet packet decomposition," in *5th Asian Control Conference*, vol. 2, pp. 1371-1376, 2004.

[11] S.G. Mallat, A Wavelet Tour of Signal Processing: The Sparse Way. Elsevier, 2009.

[12] B.M. Ebrahimi, M. Etemadrezaei, and J. Faiz, "Dynamic eccentricity fault diagnosis in round rotor synchronous motors," *Energy Conversion and Management*, vol. 52, no. 5, pp. 2092-2097, 2011.

[13] A. Ghoggal, S.E. Zouzou, H. Razik, M. Sahraoui, and A. Khezzar, "An improved model of induction motors for diagnosis purposes – Slot skewing effect and air–gap eccentricity faults," *Energy Conversion and Management*, vol. 50, no. 5, pp. 1336-1347, 2009.

[14] E.S. Obe and A. Binder, "Direct-phase-variable model of a synchronous reluctance motor including all slot and winding harmonics," *Energy Conversion and Management*, vol. 52, no. 1, pp. 284-291, 2011.

[15] H.A. Toliyat, M.S. Arefeen, and A.G. Parlos, "A method for dynamic simulation of air-gap eccentricity in induction machines," *IEEE transactions on industry applications*, vol. 32, no. 4, pp. 910-918, 1996.

[16] CEDRAT Group. *Flux2D User's Guide*. France, 2011.

[17] M. Blodt, P. Granjon, B. Raison, and J. Regnier, "Mechanical Fault detection in induction motor drives through stator current monitoring-Theory and application examples," in *Fault detection*: IntechOpen, 2010.

[18] J. Zarei and J. Poshtan, "Bearing fault detection using wavelet packet transform of induction motor stator current," *Tribology International*, vol. 40, no. 5, pp. 763-769, 2007.

IEEE Office - SEET Complex, Federal University of Technology, Owerri, Nigeria, https://aeuso.org
EISSN: 2305-0543, PISSN: 2411-6173